Mansoura Engineering Journal, (MEJ), Vol. 29, No. 1, March 2004.

STATIC AND DYNAMIC CHARACTERISTICS OF ASWAN CABLE-STAYED BRIDGE

الخواص الاستاتيكية و الديناميكية لكوبري أسوان الملجم

By

A.M. Abou-Rayan

Assistant Professor

Civil Engineering Technology Department

Banha Higher Institute of Technology

Banha Eljadida, Banha 13512

خلاصة:

تعتبر الكباري من المنشآت الحيوية للبنية التحتية في المجتمعات المعاصرة و إن التقييم الديناميكي لها يمثل أهمية قصوى. في هذا البحث تم دراسة السلوك الاستاتيكي و الديناميكي لكوبري أسوان الملجم من خلال نموذج ثلاثي الأبعاد باستخدام نظرية العناصر المحددة. تم إجراء التحليل الاستاتيكي و الديناميكي لحالة حدود التشكل و حالة حدود التشرخ. و قد تم إجراء التحليل الاستاتيكي لحالات تحميل مختلفة، أما بالنسبة للتحليل الديناميكي فقد تم استخدام نوعين من أحمال الزلازل و ذلك في الثلاث اتجاهات المتعامدة للكوبري (الاتجاه الطولي و العرضي و الرأسي). و بناء على النتائج المستخلصة فان النظام الاستاتيكي للكوبري له تأثير غالب على طبيعة و أشكال الاهتزازات للكوبري. و كذلك تبين أن قيم الترخيم القصوى تزيد في حالة حدود التشرخ مما يستلزم متابعة قيم الترخيم للكوبري بشكل دوري. و تحتوى النتائج أيضاً على الخواص الاستاتيكية و الديناميكية للكوبري.

ABSRACT

Bridges are indispensable components of the infrastructure of modern society, and their assessment via techniques of structural dynamics is assuming greater importance. The static and dynamic behaviors of the Aswan-Canal cable-stayed bridge are investigated through a three-dimensional finite-element model. These investigations were carried out under normal stage and under assumed cracking stage. Different load cases are used for the static analysis. The seismic response analyses have been conducted from the deformed equilibrium configuration due to bridge own-weight. Two earthquake records are used in the analysis.

Accepted March 31, 2004.

Each earthquake record was input in the bridge longitudinal, lateral, and vertical directions simultaneously. The results show that the bridge statical system has dominant influence on the bridge vibrations and that the bridge deflection should be monitored carefully. Also, there is a strong coupling in the three orthogonal directions within most modes of vibrations. Results include static and dynamic characteristics, time-history and frequency –domain responses.

INTRODUCTION

Since cables instead of interval piers support cable-stayed bridges, they are much more flexible than conventional continuous bridges, especially for long-span bridges. In view of the characteristics of the structural supporting conditions, bridge decks and pylons are subjected to strong axial forces (compression forces) arising from cable reactions. These axial forces cause geometric nonlinearity. In addition to the axial forces, some of the most important factors on the analysis of cable-stayed bridges are the cable nonlinearity due to its own sag, the interaction between the cables and the bridge deck, and the interaction between the cables and the pylons. A common approach to account for the sagging of inclined cables is to consider an equivalent straight modulus of elasticity, Gimsing [1].

$$E_{eq} = \frac{E}{1 + \frac{(L_o \gamma)^2}{12\sigma^3} E} \tag{1}$$

where, E_{eq}= equivalent elastic modulus of inclined cables, E = tangent modulus of elasticity for the cable, L_o = horizontal projected length of the cable, γ = weight per unit volume of the cable, and σ = cable tensile stress. The above equation gives the instantaneous tangential value of the equivalent elastic modulus that the cable tensile stress reaches. Cable arrangement can be in a single plane or double plane systems. For complete and comprehensive review of cable stayed bridges the reader is referred to Gimsing [1].

The objective of this study is to obtain a comprehensive understanding of the static and dynamic characteristics (for the normal and assumed cracking stages) of a recently completed long-span cable-stayed bridge over the Nile in Aswan, Egypt. 11 kms north of Aswan dam. The loads considered for the static analysis are the dead and live loads and for dynamic analysis are the seismic loads. The finite-element method is utilized in order to carry out this study. A three-dimensional dynamic finite-element model is first constructed for the bridge.

The bridge model is allowed to deform under its own weight to its static equilibrium before calculating any responses, static or dynamic.

DESCRIPTION OF ASWAN CABLE-STAYED BRIDGE

The target cable-stayed bridge links the east and west of the river Nile near Aswan City, playing an important role in transportation. The bridge consists of a continuous concrete deck, two hollow box-shaped towers, and one-plane semi-fan type of cables. Fig. 1 shows a schematic representation of the bridge. The bridge deck extends continuously from pier 5 at the West Side to pier 10 at the East Side, stretching an overall length of 500 m. The main span is 250 m and there are two equal side spans of 125 m each, linking the approach bridges at the East-side and the West-side, respectively; the side spans are provided with auxiliary supports P6 and P9. The bridge deck rises 13 m above the waterline. Outlines of the main bridge elements are described below, Labib and Bakhoum [2].

Bridge Deck

The bridge deck is a prestressed segmental concrete deck of a single cell trapezoidal box-girder with two inclined webs, 42 cm in thickness. The box-girder segment has a total height of 3.3m, 3.9m in length, and a 24.3 m in width. This large width could lead to a local buckling due to force interaction between the deck and cables, especially to those stay forces from 109H15-cable stay. Also, the single plane arrangement, for the cables, requires a hollow box main girder with considerable torsional rigidity in order to keep the change of cross-section deformation due to eccentric live load within allowable limits. For the aforementioned reasons, the top slab (22cm in thickness) was stiffened with double longitudinal girders in the central part of the box-girder. Also the top slab was prestressed transversally by 4F15S tendons. The bottom slab (20 cm in thickness) was transversely stiffened by 30cm deep cross-beam.

Stay Cables

A single vertical plane of 56 cables along the middle longitudinal axis of the superstructure is located in a single vertical strip. The stays are composed of 73 to 109 H15 strands surrounded by an HDPE tube (high-density polyethylene sheath). Each strand is 15.7 mm in diameter containing 7 wires. Strands are galvanized, waxed, and individually HDPE sheathed. The breaking load per wire is 265 KN. The anchorage spacing of stays on the deck is 7.812 m (i.e. every two segments).

Tower and Pier

There are two towers (west and east) and six piers. The tower is a prestressed concrete structure, fixed to the deck and has a box girder shape with outer dimensions 3mX6m and 1mX3m inner dimensions. The tower height is 55m from the deck level. The stays are anchored to the tower on a vertical range of about 30m. Looped post-tensioning tendons perform the transfer of the stay forces to the tower. The pier shaft (piers 7 &8), of pyramidal shape, is a massive reinforced concrete structure (24X25m at bottom). Each pier is founded on 88 piles of diameter 1.10m. Piers 5,6,9,and10 are reinforced concrete box-sections.

Bearings

Two lines of elastomeric bearings (8 bearings per line) are placed on top of each pier shaft (7& 8) to support the bridge deck. The bearing size is 1000X1000X160 mm. The laminated bearing is composed of a succession of steel reinforcing plates (thickness: 4mm) and elastomeric layers (thickness: 16mm). Two PTFE, 600X600X60 mm, bearings are placed on piers 5,6,9,and10 to permit longitudinal movements and to limit horizontal deflections.

Bridge statical system

Generally, in the case of single-box main-bridge system, the towers are fixed to the superstructure (rigidly connected to the deck), which is the present case under study. Towers and the bridge deck are considered to be as one structural unit, since towers are fixed to the deck. Therefore, the bridge statical system is composed of two separate structural units; 1) towers and deck, 2) piers. The first unit is rested on rubber bearings, which is fixed to the pier. This statical system is completely different than that of the Suez-Canal cable-stayed bridge. Where, the steel deck is rested on pylons (tower and pier are one structural unit) cross beams by means of rubber bearings and the other supports, near the approach bridge, are rollers.

Finite Element Model

The bridge is discretized as a three-dimensional finite-element model, which includes three types of elements: frame, shell, and cable. First, the bridge deck has been modeled as shell elements. Next, towers have been modeled as three-dimensional frame elements. Each node of both shell and frame elements incorporates six degrees of freedom, i.e., translation in the X, Y, and Z directions as well as rotation about the three directions. Last, the stayed cables have been modeled as tension-only elements. Therefore, if the cable element is subjected to compressive forces, the cable stiffness will be taken as zero. In order to effectively model the structure, material properties are assumed as follows. For concrete, the modulus of elasticity

E is 30 GPa; Poisson's ratio υ is 0.25; and the mass density is 23.2 kN/m^3. For steel, the modulus of elasticity E is 200 GPa; Poisson's ratio υ is 0.3; and the mass density is 78.6 kN/m^3. The material behavior is linearly elastic and the moduli of elasticity E in tension and compression are equal. The damping ratio was assumed constant and equal to 3%, which is the common percentage of damping in this class of bridges. The vertical and horizontal stiffness of the bearings are calculated according to the following formulas:

$$S = \frac{L}{4e}, \quad E_a \approx 6GkS^2, \quad K_V = \frac{AE_a}{L_r}, \quad K_H = \frac{AG}{L_r} \qquad (2)$$

where S = Shape factor, L_r = bearing's length, e = rubber layer thickness, E_a = apparent modulus of elasticity corrected to account for rubber compressibility, G = shear modulus, k= rubber compression modulus, K_V = bearing's vertical stiffness, and A= rubber layers cross sectional area K_H = bearing's horizontal stiffness. The damping coefficient ratio for bearing was taken 10%. The connection between the deck and piers 7 and 8 are modeled by rigid link in the vertical and horizontal directions in order to allow for the deck to move freely in the longitudinal direction and rotate freely about the transverse axes of the deck. The connections between the deck and piers 5,6,9 and 10 are modeled by swing rigid links in order to restraint the relative movement between the deck and the piers in the vertical direction. The calculated bearing's stiffness' (equation 2) are substituted for the links stiffness. A numerical analysis is carried out based on the tangent stiffness method and modal superposition.

STATIC ANALYSIS

Different standard bridge loading-patterns are adopted in the analysis. The loading patterns considered are illustrated in Fig. 1. It should be mentioned that, bridge own-weight is considered in all patterns (live load considered = 4kN/m^2). Fig. 2 shows a schematic representation for the static deflection due to the bridge own-weight and prestressing forces. The static deflection under own weight was found to be 49 cm at the center of the main span. The maximum deck deflection values at the center of the main span for all loading cases are shown in Fig.3. It is obvious that the maximum contribution comes from the bridge own-weight and that the maximum deck deflection occurs due to load case 1. It is worth mentioning that for load cases 3 and 5 the deck deflection is less than that of the bridge own-weight only. This is due to the fact that the loading for these two cases is on the side span only. Fig. 4 shows the variations of cables, for the west tower, tension force due to different load cases. It is shown that cables tension decreases to a very small value near the tower.

which is the usual pattern for these types of structures. In cable stayed bridges when no auxiliary support (piers 6&9) in the side span exist, cables tension have decreasing values near the tower and an increasing values away from the tower to a maximum value (so called V shape around the tower. Abou-Rayan and Seleemah [3]). In our case, the existence of auxiliary support, pier 6, repeats the aforementioned pattern, the first one around pier 6 and the second one around the main support pier 7. It should be mentioned that the pattern is not symmetric around the tower since there is no auxiliary support at the main span. Based on Fig. 4, it can be concluded that: 1) the bridge own-weight contributes to about 80% of the total tension force, 2) the least tension force occurred due to load case 5, and (3) the maximum cables tension force occurred due to load case 1.

Cables with different locations are inclined at different angles to the tower and the axial cables tension forces are transformed from the vertical components of the cable reaction to the tower inducing compression forces on the tower. Distribution of compression forces on the west tower is shown in Fig. 5. The maximum compression force occurred due to load case 1, since it is the maximum case for the cables tension force. The compression forces accumulate to its maximum value of 280 MN. It is seen that the accumulation rate is linear up to a tower height of 30 m (from top to bottom), where after that the rate decreases suddenly since the last two cables (601, 602) have very small tension forces; thus, their contribution to the accumulated compression force is very small. Also, from height 25m and below the compression forces become constant (cable 601 connected to the tower at 25m height). Fig. 6 shows the distribution of shear forces (the horizontal component of the cable tensile force) on the west tower. The maximum shear forces, 14 MN, occur at 50m and 32m heights due to load case 1, whereas the minimum shear is due to load case 4, where no loading at the side span. The shear force changes sign at the tower-cable connection, cable 609, at a height of 42m; this cable is connected from the other end to the deck at pier 6, at joint 207. The shear force is constant from the deck level up to a tower height of 25m, since there are no cables connected at this range. The west and east towers deformations are shown in Fig. 7. The maximum value of side-sway displacement is approximately 14cm at the top of the tower. For all load cases the side-sway displacement is to the right for the west tower and to the left for the east tower, since the bridge own-weight contribution overcomes any load case (this is true only for the static loads).

From the previous results it is clear that the bridge own-weight has the greatest contribution for all straining actions. Also, the full span loading is quit enough for the preliminary analysis.

DYNAMIC ANALYSIS

In recent investigations [4-7] concerning the dynamic analysis of cable-stayed bridges, it was assumed that only one earthquake component shacks the bridge at the supporting points. Therefore, there is an urgent need for more comprehensive investigations of seismic analysis of cable-stayed bridges taking into account a three-directional ground shaking excitations simultaneously. To evaluate the different dynamic characteristics of the bridge, two different earthquake records, Elecentro and Taft with three components for each, are considered separately. Analysis was carried out in both time and frequency domains. It should be noted that all analyzes started from the deformed equilibrium configuration due to bridge own-weight. Since there is a tremendous amount of results, only key response results will be considered.

Equation of Motion

The dynamic equation of motion of three-dimensional vibration of the bridge when subjected to seismic excitations at all supports can be written as, Clough and Penzien [8]:

$$M\ddot{V}_t + M\ddot{V}_g + C\dot{V}_t + C_g\dot{V}_g + KV_t + K_g V_g = 0 \qquad (3)$$

where M, C, and K = the mass, damping, and tangent stiffness matrices of non-active degrees of freedom of the bridge; M_g, C_g, and K_g = the mass, damping, and tangent stiffness matrices of the active degrees of freedom of the bridge (corresponding to the point of ground motion applications, supports); V_t =total nodal displacement; and V_g = displacement resulting directly from the support motions. Equation (3) can be written in a partition form as. Bake and Loodno [9]:

$$\begin{bmatrix} M_{bb} & M_{bg} \\ M_{gb} & M_{gg} \end{bmatrix}\begin{Bmatrix} \ddot{V}_b \\ \ddot{V}_g \end{Bmatrix} + \begin{bmatrix} C_{bb} & C_{bg} \\ C_{gb} & C_{gg} \end{bmatrix}\begin{Bmatrix} \dot{V}_b \\ \dot{V}_g \end{Bmatrix} + \begin{bmatrix} K_{bb} & K_{bg} \\ K_{gb} & K_{gg} \end{bmatrix}\begin{Bmatrix} V_b \\ V_g \end{Bmatrix} = \begin{Bmatrix} 0 \\ 0 \end{Bmatrix} \qquad (4)$$

where, the subscript g designates the degrees of freedom corresponding to the points of application (active) and directions of ground motion; and the subscript b designates all other structural degrees of freedom of the bridge. Thus, the matrices M_{bg}, C_{bg}, and K_{bg} are the rectangular mass, damping, and stiffness matrices, respectively, which represent the coupling between the structure nodes not connected to the ground (non-active) and the support

displacements due to ground motion. The total nodal displacement may be decomposed into quasi-static displacement and vibrational displacement. The solution of equation (4) can be written as:

$$\begin{Bmatrix} V_b \\ V_g \end{Bmatrix} = \sum_{i=1}^{l} \begin{Bmatrix} S_{bi} \\ \delta_{gi} \end{Bmatrix} f_i(t) + \sum_{n=1}^{p} \begin{Bmatrix} \phi_n \\ 0 \end{Bmatrix} q_n(t) \tag{5}$$

where S_{bi} is the ith quasi-static function that results from unit displacement in the ith degree of freedom at the supporting point; $f_i(t)$, $i=1,2,....,l$ = the input displacement ground motions to the supporting points of the bridge in the three orthogonal direetions; δ_{gi} = vector of which the ith element is equal to unity, with all its other elements being zero; $\{\phi_n\}$ = the nth free vibration mode shape of the bridge with all support-point displacement constrained; $q_n(t)$ = the nth generalized coordinate; and p = the number of mode shapes used in the modal analysis.

Dynamic Characteristics of the Free Vibration of the Bridge

Unlike the classical suspension bridges, vibrations of cable-stayed bridges cannot be categorized as vertical, lateral, and longitudinal. The response of this type of bridge to earthquake excitations has special features due to the complicated interaction of the three-dimensional input motions with the whole structure, Bruno and Leonardi [10]. Fig. 8 shows the lowest 12 mode shapes only. Periods, frequencies, and mode shape types are tabulated in Table 1. As seen from the figure, mode shapes can be categorized into three types, towers-, deck-, and coupled-modes. Towers-modes (lowest mode shapes), which, have very low frequencies (long periods) are dominated by towers swaying in lateral direction (Y). The first mode is for the towers swaying in phase while the second one is for the towers swaying out-of-phase. The deck modes are dominated by the lateral sway in the horizontal plan. The third mode is close to half sine wave and the fourth one is antisymmetrical (one sine wave). The rest of the modes are coupled with vertical vibrations of the deck and torsional vibration of the towers and deck. From the aforementioned mode shapes it clear that the bridge statical system has a dominant effect on the bridge vibrations. When tower are and pier constitute one structural element, pylon. as in the case for the Suez-Canal cable-stayed bridge where roller supports exist. lowest mode shapes are for the deck in the longitudinal direction. see Abou-Rayan [11].

Dynamic Characteristics of the Seismic Induced Vibration of the Bridge

Peak accelerations of the seismic excitations used in the dynamic analysis. are given in Table 3. Fig. 9 illustrates some of the calculated displacement time histories. By examining these

figures, it can be seen that the excitations can have a significant effect on the response displacement at the flexible parts (towers) of the structure, especially for the flexible directions (compare joints 79,207, and 233 in Y-direction with all other directions). Since the responses due to Taft records are small compared to other responses due to Elcentro record, all responses were normalized for the sake of comparison between responses (i.e., responses magnitudes were calculated from the bridge equilibrium configuration). For joint 207 the displacement in the vertical direction, Z-direction, is minimum, almost zero. This behavior is normal since joint 207 is a support joint (connected to pier 6). For joint 79, the side-sway motion of the tower is in the lateral direction, Y-direction. This is in agreement with mode shapes of the structure, modes 1 and 2. The following tower response characteristics are evident from the figures:

1- The motion is partially restrained in the X-direction because of the cables (i.e., the lowest displacements time histories are in the longitudinal-direction).
2- The tower stiffness, in the y-direction, is less than the deck stiffness and the motion has very low frequency, 0.076 Hz.
3- Time history response pattern for the lateral direction, joint 79, is completely different from any other response pattern previously discussed. It is clear from the figure, that the amplitude rate change (zero-crossing rate) is slower than all other patterns, i.e., the period is lengthened. This means that the time history response is close to a semi periodic motion with longer period in that direction.
4- This response pattern is a consequence of the structure statical system concerning the tower, deck, and pier connections (it was shown that the difference between the period of the first two modes and the other modes is large, see table 1).

The Spectral acceleration for joints 79, 207, and 233 due to both earthquakes are shown in Fig.10. The following response characteristics are evident from the Figure:

1- There is a multi-modal contribution to each response quantity. These contributions are more pronounced in the high frequency (small-period) range of the response.
2- The high occurrence possibilities of low frequency modes (long periods), in general, for any structure are for the first modes, 1, 2, 3, and 4. At these period ranges (3-13 seconds) the spectral accelerations have zero values. In other words, the bridge responses are far away from any resonance phenomena to occur.

3- Generally, the wind forces have high frequencies. Accordingly, no threat to the tower stability is expected. Since the dominant mode shapes have low frequencies (long periods).

4- For joint 79 the spectral acceleration of the lateral motion is very small, whereas the maximum peak occurs for the vertical direction, which has the smallest time-history response.

Some selected member-forces time histories are calculated and plotted to give a representative picture of the models' response to seismic excitation, Fig. 11. Cables axial forces are defined in the local coordinates of the specific cable. It is evident from examining these plots that the seismic excitations have an extremely strong influence on the magnitude as well as the frequency content of the responses. It is obvious that cables on the left and on the right of the tower can be classified into three groups in terms of axial force magnitude (quantitatively). The first four cables from the top constitute the first group with high tensile forces. The next five cables constitute the second group with relatively medium tensile forces. The rest of the cables (not shown, six cables on the left and right of the tower) have small tensile force magnitude reaching a very small value for the nearest cable to the tower. In other word, cables tension force is directly proportional to the distance from the tower.

Fig. 12 shows the base-shear time history under both inputs for all directions. Despite the fact that the horizontal components for both records are higher than the vertical ones, the energy output in the vertical direction is higher than the other directions. Thus, the earthquake record with largest peak acceleration magnitude does not necessarily induce the greatest maximum response. Clearly higher mode contributions are observed in the X-direction only.

BRIDGE BEHAVIOR UNDER CRACKING STAGE

Occasionally structures are subjected to over loads beyond the point of cracking "hair cracks". One of the factors that could lead to this cracking stage is an earthquake. Therefore, the bridge main characteristics were investigated for static load and seismic forces (Elcentro) assuming hair cracks exist. While there is a tremendous amount of results, only main response results will be discussed here. These are:

a) Static deflection due to load case 1.

b) Towers displacements due to load case 1.

c) Mode shapes

d) Spectral acceleration for joint 79.

The aforementioned investigation was carried out the same as before, except that when computing the stiffness coefficients for equation (4) I_e (effective moment of inertia for computation of deflection) was substituted for I_g (moment of inertia of gross concrete section). Equation (4-62) from Egyptian Code [12] was used to compute I_e

The maximum deck deflection was found to be 59 cm, see case-1C, at the center of the main span, corresponding to 53.47 cm for normal stage. This increase in the deck deflection leads to increase in towers side-sway displacement by about 4cm at the top, see figure 7 case-1c. Despite the fact that the bridge deck and towers are subjected to strong axial compression forces, these deflection increases could lead to an overall instability for the structure. Also this could lead to damage in the cables connections either to the tower or the deck.

It is clear from table 2, that the bridge natural modes were not affected much by the assumed cracked state. Natural periods for this case are longer by about 0.6 Sec. and mode shapes characteristics are the same. This behavior is excepted since the main factors affecting these mode shapes are the bridge statical system and the rubber bearings, isolation system. By examining Fig. 10(a), it is clear that the peak of the spectral acceleration for joint 79 for the cracked stat, 79-Zc is lower than the corresponding one, 79-Z. This is in agreement with mode shapes results for the cracked state (natural periods are longer especially for the tower modes).

AS seen the cracking stage analysis shows that the deflection increased than expected. This deflection could increase with time, which leads to undesired consequences, and to an overall stiffness decrease for the bridge.

CONCLUSIONS AND RECOMMENDATIONS

The static and dynamic characteristics of Aswan Cable-Stayed Bridge are investigated, through finite element analysis. Based on this investigation, the following conclusions and recommendations can be made:

1- From the static analysis it is clear that the bridge own weight contribution to the response represents about 80% of the total response. Maximum straining actions are due to full span loading; in other word, the full span loading is quit enough for the preliminary analysis.

2- The bridge statical system has a significant effect on the overall bridge behavior. Therefore, for this type of bridges an investigation concerning the tower-deck connection should be conducted (i.e., tower fixed to the deck and tower fixed to the pylon).

3- For this three-dimensional structure, there is strong coupling in the three orthogonal directions within most modes of vibration. Therefore, a two-dimensional dynamic assessment is not adequate for this type of structures.

4- The assumed case of hair cracks existence did not affect the main bridge characteristics except for the increased deflection in the deck and towers. . This deflection could increase with time, which leads to undesired consequences, and to an overall stiffness decrease for the bridge. Therefore, it is strongly recommended that the bridge deflections (deck and towers) must be monitored continuously so that, any deflection increase than expected could be an alarm or hair cracks existence. Also, overall bridge stability should be thoroughly investigated under this assumption. Based on these results, it is believed that the hair cracking stage was not considered in the original bridge analysis.

5- It would have been better if the main span was 400m instead of 250, which is considered small compared to the existing concrete cable-stayed bridges (existing bridges reached more than 400m for main span). This would have given clear navigation stream (Nile River width at the bridge site is about 400m) and have also eliminated the cost of constructing the cofferdams for piers 7 and 8.

Although this study has predicted that the bridge is safe against wind forces, it is recommended to investigate the bridge characteristics under high wind speed. Also, The use of stochastic methods for dynamic analysis (random vibrations) to predict the earthquake-response of such bridge is recommended. This can allow for studying the effects of support-excitation, cross-correlation, and modal cross-correlation on the bridge responses. The effect of soil-structure interaction, and local soil conditions at the site of the bridge on the dynamic characteristics and earthquake-responses of the bridge should be investigated.

ACKNOWLEDGEMENT

The author wishes to express his appreciation to Professor A. Mahfouz for his valuable comments, which enriched this study.

REFERENCES

1. Gimsing, N. J., **Cable supported bridges: concept and design**, Wiley New York, 1983.
2. Labib, S., and Bakhoum, M., "Aswan Bridge Over The Nile," Proceedings of the Bridge Engineering Conference 2000, (ESE) Sharm El-Sheik, Egypt, 2, 2000, 601-608.
3. Abou-Rayan, A.M., and Seleemah, A.A., "Cable-Stayed Bridges - Parametric Analysis." Civil Engineering Research Magazine, Al-Azhar University, 23, 1, 2001, 146-156.
4. Moon, S. J., Bergman, L. A., and Voulgaris, P. G., "Sliding Mode Control of Cable-Stayed Bridge Subjected to Seismic Excitation," Journal of Engineering Mechanics, 129, 1, 2003, 71-78.
5. Chang, C. C., Chang, Y. P., and Zhang, Q. W., "Ambient Vibration of Long-Span Cable-Stayed Bridge," Journal of Bridge Engineering, 6, 1, 2001, 46-53.
6. James, M. W., Brown, J., and Pin-Qi X., " Dynamic Assessment of Curved Cable-Stayed Bridge by Model Updating." Journal of Structural Engineering, 126, 2, 2000, 252-260.
7. Ren, W., "Elastic-Plastic Seismic Behavior of Long Span Cable-Stayed Bridges," Journal of Bridge Engineering, 4, 3, 1999, 194-203.
8. Clough, R. W., and Penzien, J., **Dynamics of structures**, McGraw-Hill, New York, N.Y., 1975.
9. Bake, N. C., and Loodno, B. J., "Seismic Study of Cable-Stayed Bridge." Structures Congress 94, Atlanta, Gorgia, April 24-28, 1994, 1197-1207.
10. Bruno, D., and Leonardi, A., "Natural Periods of Long-Span Cable-Stayed Bridges." Journal of Bridge Engineering, 2, 3, 1997, 105-115.
11. Abou-Rayan, A.M., "Three-Dimensional Nonlinear Seismic Behavior of Suez-Canal Cable-Stayed Bridge." Proceedings of the 4th International Conference on Civil and Architecture Engineering, Military Technical College, Cairo, 14-16 May 2002, 1-12.
12. The Egyptian code committee, **The Egyptian Code For Design And Construction of Concrete Structure**, ECCS 203-2001.
13. Ren, W., "Ultimate Behavior of Long-Span Cable-Stayed Bridges." Journal of Bridge Engineering, 4, 1, 1999, 30-37.

14. Yang, F., and Founder, G. A., "Dynamic Response of Cable-Stayed Bridges Under Moving Loads." Journal of Engineering Mechanics, 124, 7, 1998, 741-747.

15. Astaneh-Asl, A., and Black, R. G., "Seismic and Structural Engineering of a Curved Cable-Stayed Bridge," Journal of Bridge Engineering, 6, 6, 2001, 439-450.

16. Zhang, Q., Chang, T., and Chang, C., "Finite-Element Model Updating For The Kap Shui Mun Cable-Stayed Bridge." Journal of Bridge Engineering, 6, 4, 2001, 285-293.

Table 1: Summary of Mode Shapes

Mode	Frequency (Hz)	Period (Sec.)	Nature of Mode Shape		
			Tower	Deck	Remarks
1	0.076	13.064	LT	-----	Tower modes
2	0.078	12.693	LT	-----	
3	0.282	3.544	-----	LT	Deck modes
4	0.324	3.079	-----	LT	
5	0.537	1.862	LT	V-T	Coupled modes
6	0.598	1.671	L	V	
7	0.800	1.249	LT-T	LT-T	
8	0.809	1.235	T	T	
9	0.859	1.163	L-T	V-L	
10	1.291	0.774	L-T	V-L	
11	1.449	0.761	T-LT	T-LT	
12	1.312	0.690	L-T	L-V	

Table 2: Summary of Mode Shapes under cracking-stage

Mode	Frequency (Hz)	Period (Sec.)	Nature of Mode Shape		
			Tower	Deck	Remarks
1	0.073	13.64	LT	-----	Tower modes
2	0.075	13.203	LT	-----	
3	0.255	3.924	-----	LT	Deck modes
4	0.287	3.479	-----	LT	
5	0.462	2.162	LT	V-T	Coupled modes
6	0.552	1.810	L	V	
7	0.746	1.340	LT-T	LT-T	
8	0.778	1.285	T	T	
9	0.798	1.253	L-T	V-L	
10	1.144	0.874	L-T	V-L	
11	1.175	0.851	T-LT	T-LT	
12	1.315	0.760	L-T	L-V	

Where, V = Vertical, L = Longitudinal, LT = Lateral, and T = Torsional.

Table 3: Seismic Ground Motion Records

Seismic Records	ELCENTRO-1940 California, USA			TAFT-1952 Cincinnati, USA		
Component	S00E	N90W	Vert.	N21E	S69E	Vert.
Peak Acc.,g	0.348	0.214	0.21	0.156	0.179	0.105

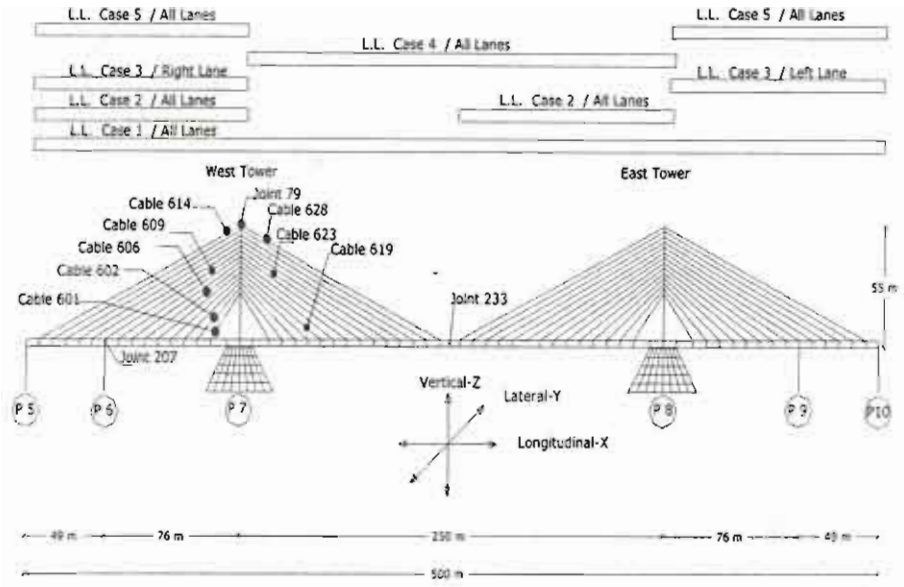

Fig. 1: Schematic representation of the bridge with loading cases.

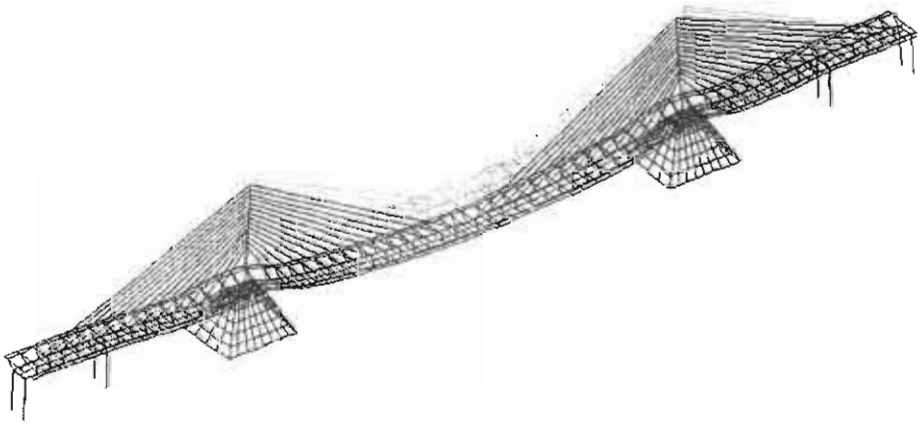

Fig. 2: Schematic representation of the static deflection due to the bridge own weight.

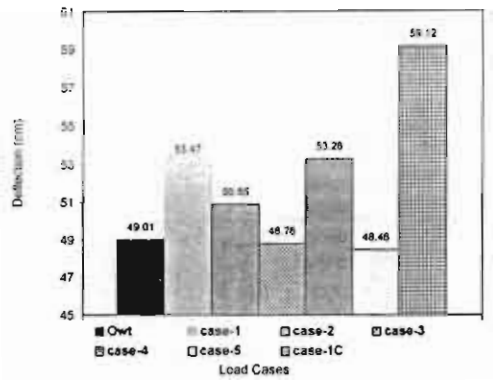

. Fig 3: maximum deck displacements at the main

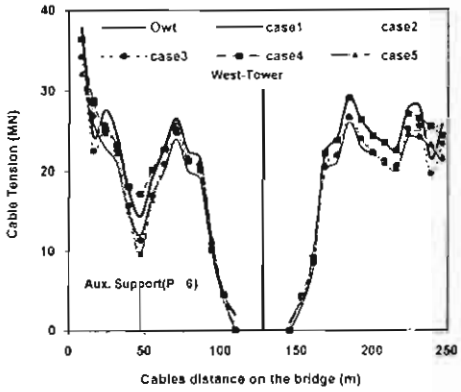

Fig. 4: Distribution of cable tension forces for the

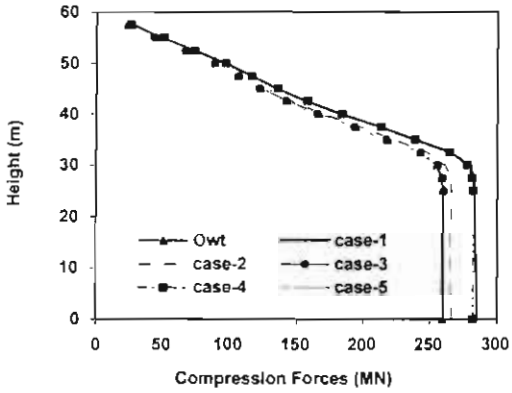

span center

Fig. 5: compression forces on the west tower

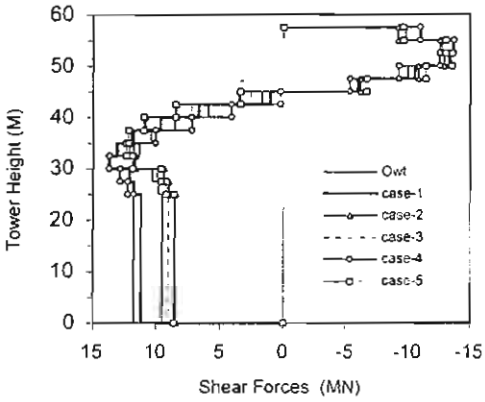

west tower

Fig. 6 : Distribution of shear forces on west tower

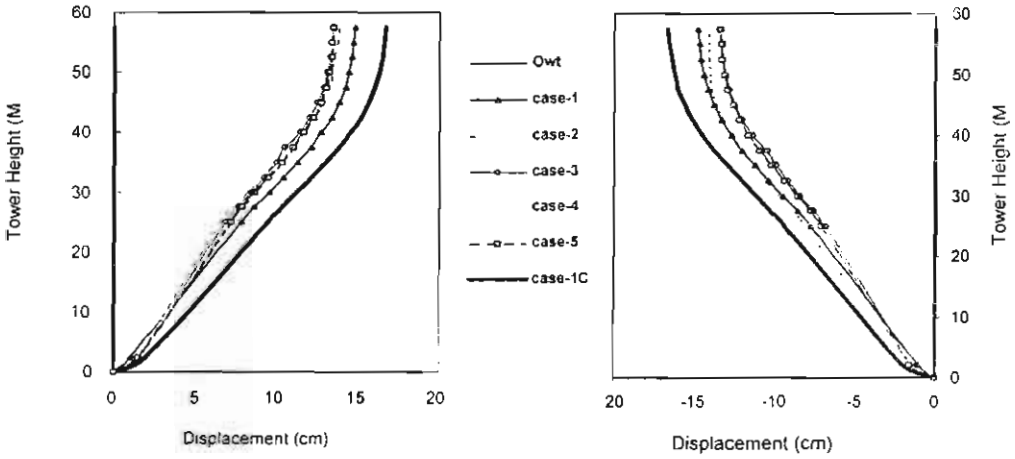

West Tower East Tower

Fig. 7: Towers deformations

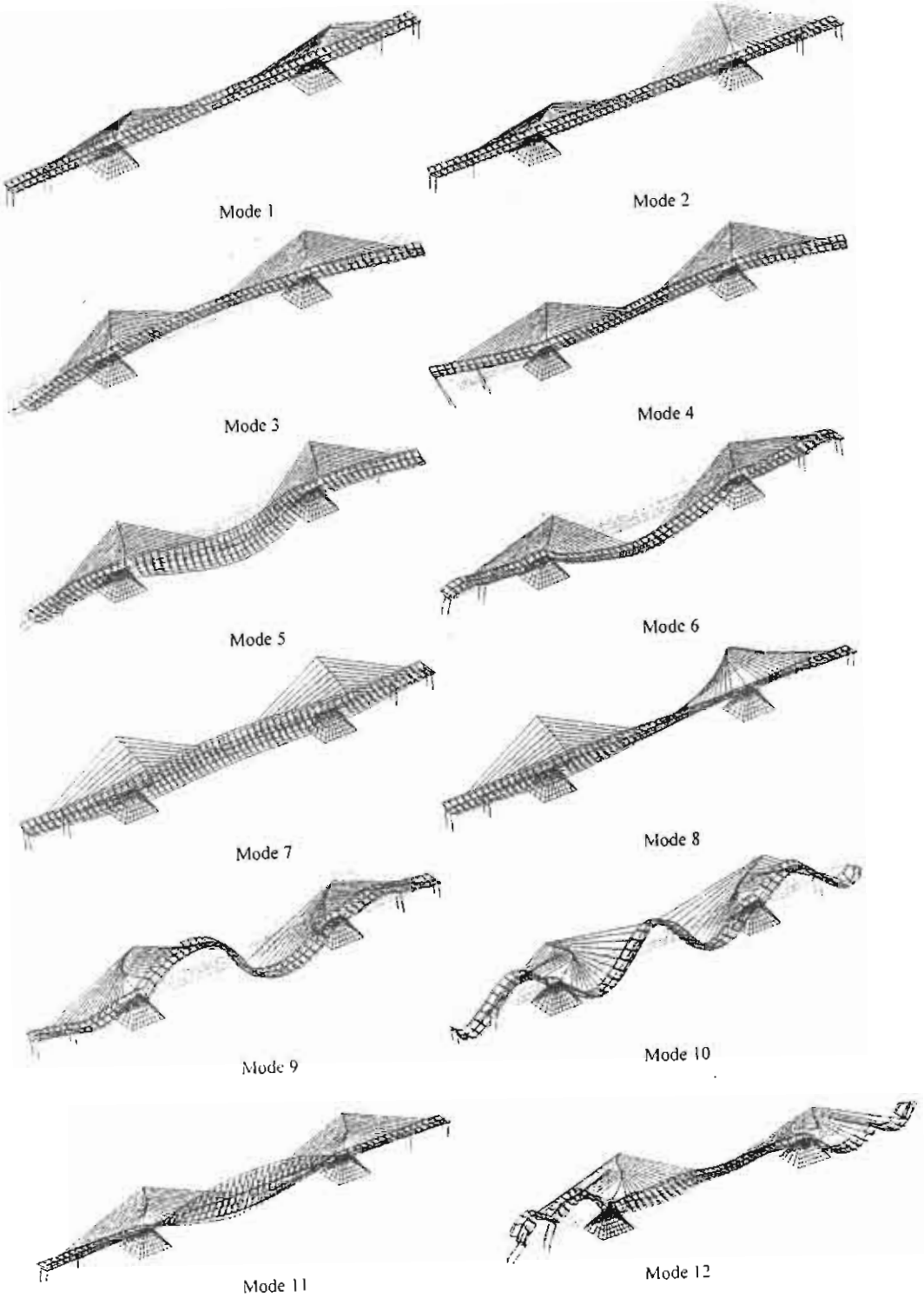

Fig. 8: Lowest 12 Mode Shapes

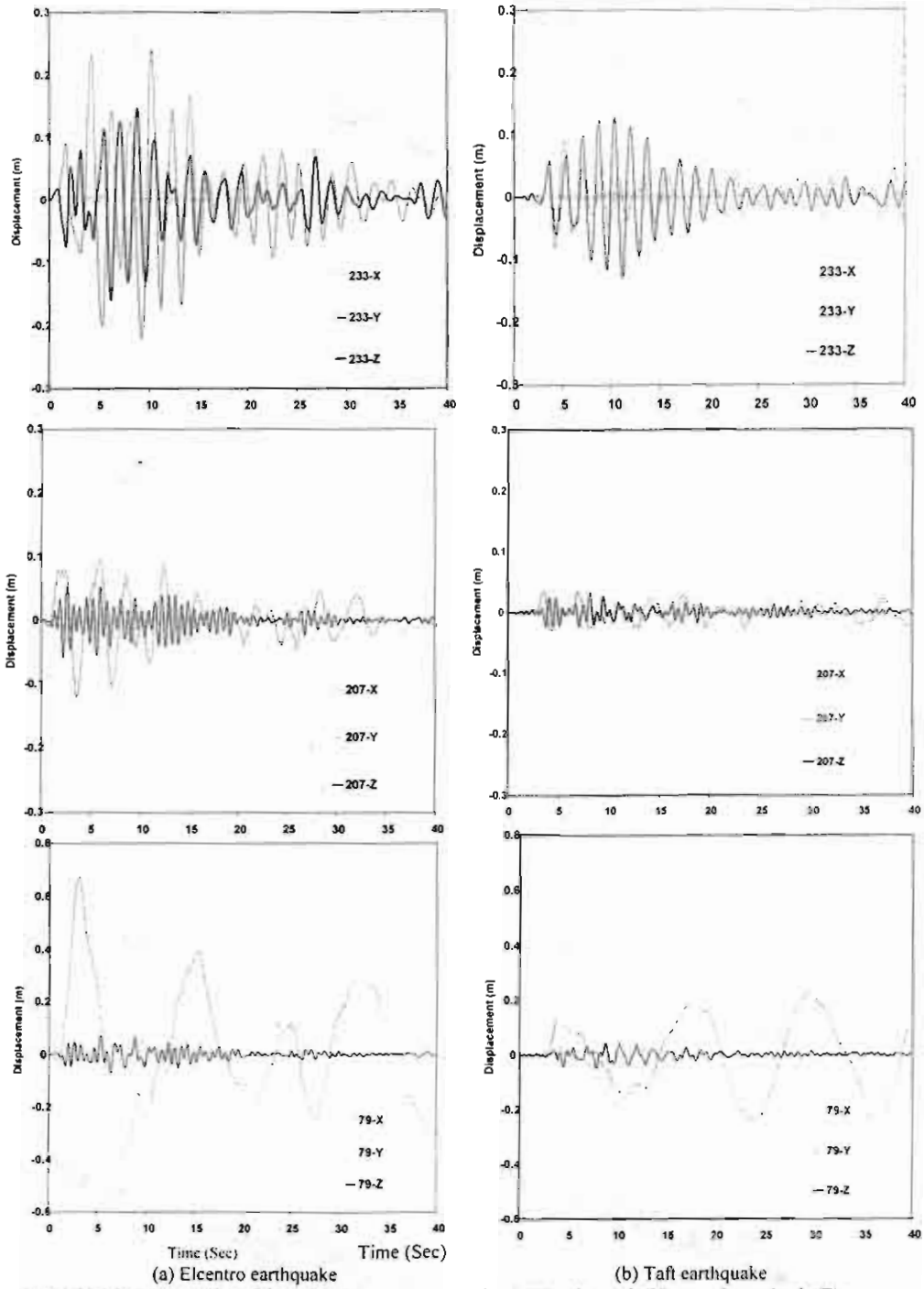

(a) Elcentro earthquake (b) Taft earthquake

Fig. 9: Displacement time histories in the longitudinal (X)-, lateral (Y)-, and vertical (Z)-directions for joints 233, 207, and 79 due to earthquake excitations.

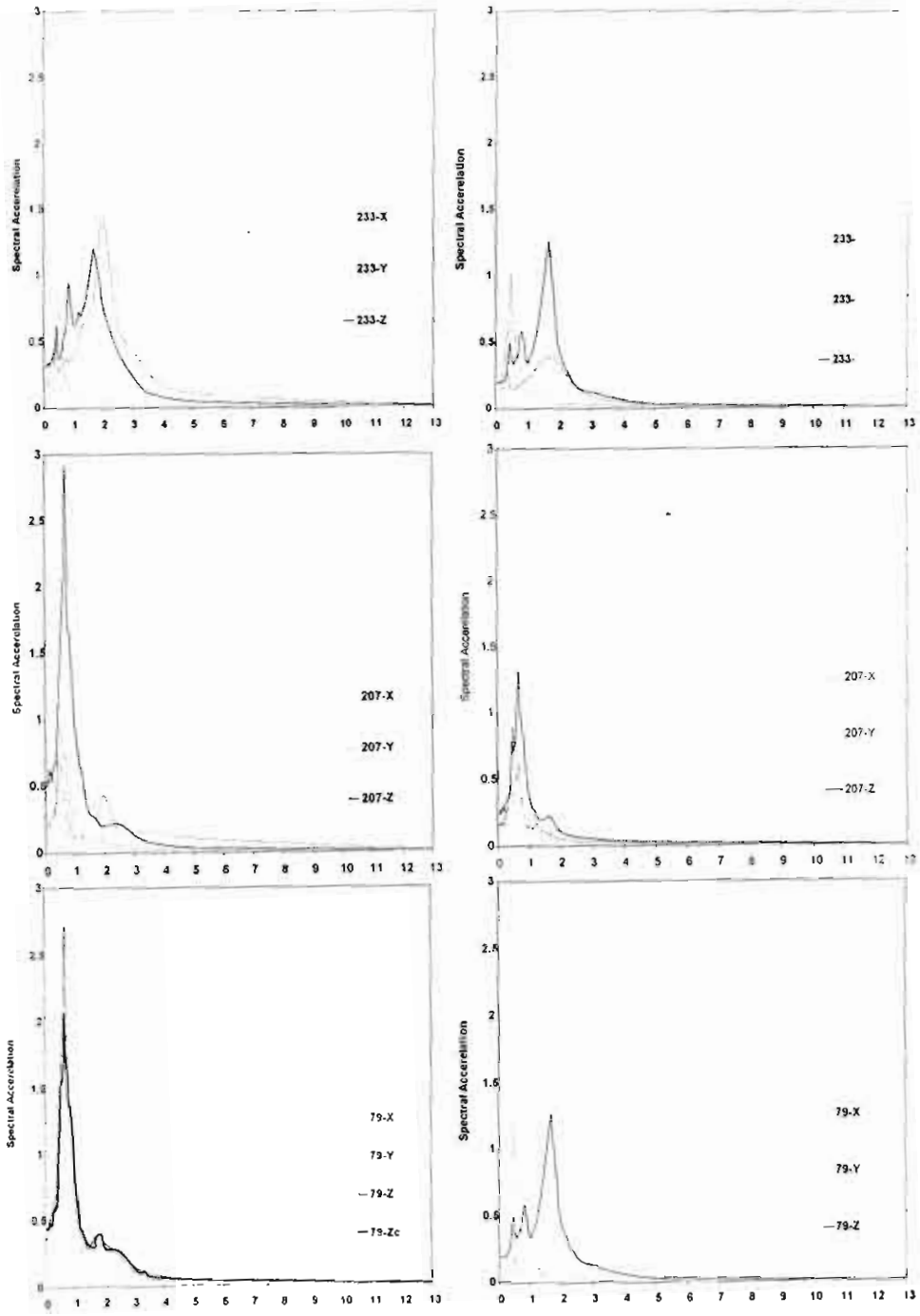

Period (Sec)
(a) Elcentro earthquake

Period (Sec)
(b) Taft earthquake

Fig. 10: Spectral acceleration VS period in the in the X-, Y-, and Z-directions.

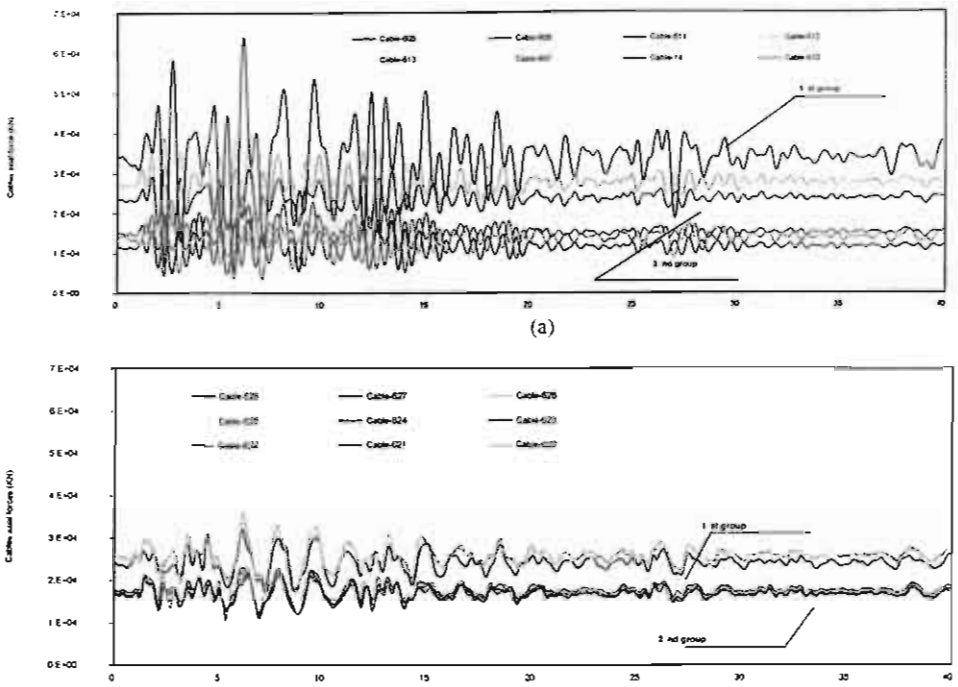

Fig. 11: Time histories for cables axial forces, (a) left of the tower, (b) Right of the tower

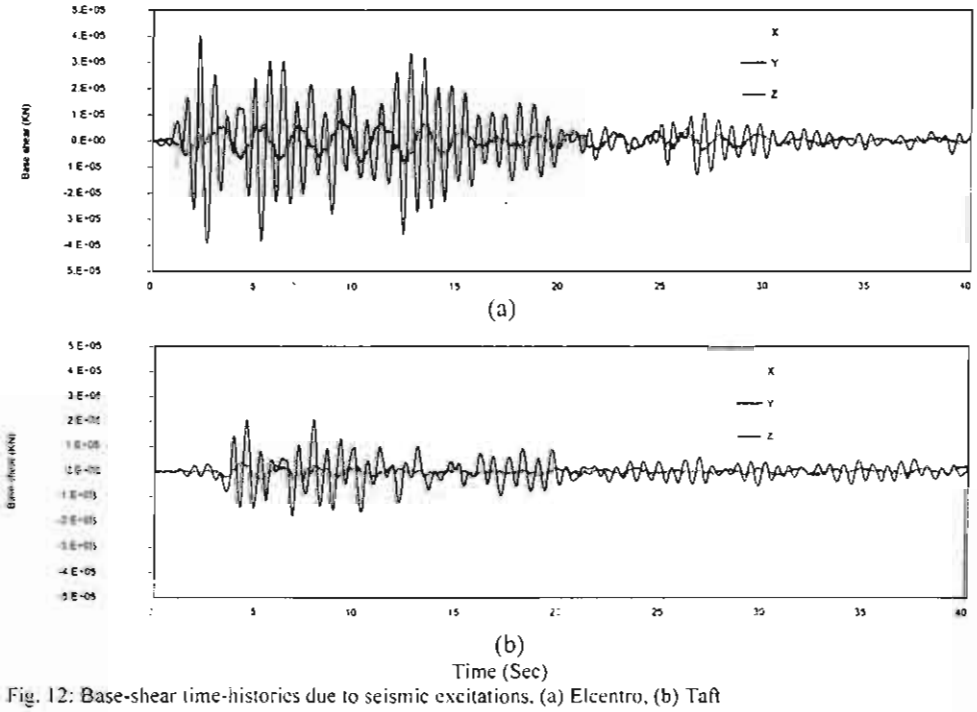

Fig. 12: Base-shear time-histories due to seismic excitations, (a) Elcentro, (b) Taft